Nonlinear dynamics of a positive hybrid observer for the impulsive Goodwin's oscillator: a design study

Nonlinear dynamics of a positive hybrid observer for the impulsive Goodwin's oscillator: a design study

Diana Yamalova*, Alexander Medvedev*, Zhanybai T. Zhusubaliyev**, and Anton V. Proskurnikov***

Abstract— **The impulsive Goodwin oscillator (IGO) is nowadays an established mathematical model of pulsatile regulation that is suitable for e.g. capturing non-basal regulation of testosterone, cortisol, and growth hormone. The model consists of a continuous linear time-invariant block closed by a nonlinear pulse-modulated feedback. The hybrid closed-loop dynamics are highly nonlinear. The endocrine feedback is biologically implemented by the bursts of a release hormone secreted by the hypothalamus and not accessible for measurement. This poses a particular state estimation problem, where both the continuous states of the IGO and the firings of the impulsive feedback have to be reconstructed from the continuous outputs, i.e. the hormone concentrations measurable in the blood stream. A hybrid observer with two output error feedback loops, one for the continuous state estimates and another for the discrete one, is considered. Positivity of the observer estimates is demonstrated. The observer design problem at hand is, for all feasible initial conditions, to guarantee the asymptotic convergence of the observer estimates at highest possible rate to the state vector of the IGO. To solve the design problem, bifurcation analysis of the observer dynamics is performed and the basin of attraction for the stationary solution with a zero state estimation error is evaluated. The observer convergence rate is evaluated through the largest Lyapunov exponent. The efficacy of the design approach is confirmed by simulation.**

I. INTRODUCTION

Biological systems often exhibit multiscale dynamics featuring both slow and fast motions. These can be captured by a combination of continuous-time blocks describing the processes that evolve slowly and instantaneous impulses portraying discrete events [1]. Theory of impulsive systems is well established [2], [3], however, the problem of state estimation in such systems remains mainly uncovered.

A simple but meaningful example of a hybrid model with applications in life sciences is the impulsive Goodwin's oscillator (IGO) [4]. It generalizes the classical continuous Goodwin's oscillator [5]–[7] by substituting the nonlinear continuous feedback of the model with a pulse modulator (being a nonlinear operator on the system's trajectories). The IGO is among few closed-loop dynamical models that have been validated on endocrine data [8], [9].

D. Yamalova and A. Medvedev were partly supported by Grant 2015-05256 from the Swedish Research Council. A. Proskurnikov was supported by Russian Foundtaion for Basic Research grant 18-38-20037.

*Systems and Control, Department of Information Technology, Uppsala University, Box 337, SE-75 105, Uppsala, SWEDEN. {diana.yamalova,alexander.medvedev}@it.uu.se

**Department of Computer Science, Southwest State University, 50 Years of October Str. 94, 305040, Kursk, RUSSIA. zhanybai@hotmail.com

***Department of Electronics and Telecommunications, Politecnico di Torino, Turin, ITALY, and Institute for Problems in Mechanical Engineering, Russian Academy of Sciences, St. Petersburg, RUSSIA anton.p.1982@ieee.org

Unlike the classical Goodwin model, the IGO has no equilibria and mostly exhibits periodic solutions, while also possessing quasiperiodic and chaotic ones [10]. In biology, all types of oscillations have to be considered since it is virtually impossible to distinguish between a perturbed periodic signal and a chaotic one in experimental data, [11].

When estimating inherently positive quantities, it is desirable to guarantee the positivity of estimates an observer produces. The problem of a positive observer design for a positive system has been thoroughly studied in the linear case [12], [13], whereas nonlinear positive observers have only been devised for special cases [7], [14]. In Luenberger-type observers, a certain conflict arises between positivity of the observer estimates and assigning a convergence rate to the state estimation error. This is natural, since the observer has to rely on the plant model to enforce positivity and the plant nonlinearity has to be essentially canceled to achieve an arbitrary fast observer convergence.

The problem of state reconstruction in oscillators can be recast as output synchronization of the observer ("slave") with the plant ("master"). Perfect synchronization corresponds to zero output error, which, given detectability of the system/solution, implies that the plant state is reconstructed. The state estimation of the IGO's hybrid dynamics boils down to the synchronization of the impulsive feedback firing sequence with that of the observer [15]. With synchronized firing sequences, the estimates of the continuous IGO states will follow, when the plant model is certain. The highly nonlinear nature of synchronization problems in impulsive systems limits the applicability of analytical observer design techniques and the observer properties are studied locally with respect to a particular solution manifold.

The present paper advocates the use of bifurcation analysis for hybrid observer design. Two observer output error feedback gains, one for the continuous state estimates and another for the discrete one, are considered as bifurcation parameters to discern nonlinear phenomena in the observer dynamics and select suitable gain intervals. Further, the gain values yielding the desired attractivity of the synchronous mode and highest convergence rate are selected for the observer implementation. The contribution to the IGO state observation problem is twofold. First, the positivity of the observer estimates is highlighted. Second, the bifurcation analysis is demonstrated to solve the observer design problem by yielding suitable values of the feedback gains.

The paper is organized as follows. First, the equations of the IGO and a previously studied hybrid observer structure with two design degrees of freedom are provided. Then,

the observer design problem at hand is stated. A discrete mapping describing the state estimate propagation from one firing of the impulsive feedback to the next one is considered to facilitate the oncoming numerical analysis. Further, a detailed bifurcation analysis of the observer dynamics is performed. Finally, an observer design algorithm is proposed and illustrated by numerical calculations and simulation.

II. The impulsive Goodwin's oscillator

The continuous part of the IGO is given by

$$\begin{aligned} \dot{x}_1(t) &= -b_1 x_1(t), \\ \dot{x}_2(t) &= g_1 x_1(t) - b_2 x_2(t), \\ \dot{x}_3(t) &= g_2 x_2(t) - b_3 x_3(t), \end{aligned} \tag{1}$$

where $x_1(t)$ undergoes jumps[1] at the time instants t_n, $n > 0$:

$$\begin{aligned} x_1(t_n^+) &= x_1(t_n^-) + \lambda_n, \quad t_{n+1} = t_n + T_n, \\ \lambda_n &= F(x_3(t_n)), \quad T_n = \Phi(x_3(t_n)). \end{aligned} \tag{2}$$

respectively. Model (1),(2) can be rewritten as

$$\begin{aligned} &\dot{\mathrm{x}}(t) = A\mathrm{x}(t), \quad \mathrm{y}(t) = L\mathrm{x}(t), \quad z(t) = C\mathrm{x}(t), \\ &\mathrm{x}(t_n^+) = \mathrm{x}(t_n^-) + \lambda_n B, \quad t_{n+1} = t_n + \Phi(z(t_n)), \\ &\lambda_n = F(z(t_n)), \quad n = 0, 1, 2, ..., \end{aligned} \tag{3}$$

where the vectors and matrices are as follows,

$$A = \begin{bmatrix} -b_1 & 0 & 0 \\ g_1 & -b_2 & 0 \\ 0 & g_2 & -b_3 \end{bmatrix}, \; B = \begin{bmatrix} 1 \\ 0 \\ 0 \end{bmatrix}, \; L = \begin{bmatrix} 0 & 1 & 0 \\ 0 & 0 & 1 \end{bmatrix},$$
$$C = [0 \quad 0 \quad 1], \quad \mathrm{x} = [x_1, x_2, x_3]^\top.$$

The discrete part of the IGO described by (2) implements a pulse-modulated feedback over the continuous dynamics of (1), where $F(\cdot)$ is the amplitude modulation function and $\Phi(\cdot)$ is the frequency modulation function. The modulation functions are nonlinear, positive, and bounded; $F(\cdot)$ is decreasing and $\Phi(\cdot)$ is increasing. To be more concrete, they are assumed to be Hill functions of order β in the form:

$$\Phi(x_3) = \Phi_1 + \Phi_2 \frac{(x_3/h)^\beta}{1 + (x_3/h)^\beta}, \quad F(x_3) = F_1 + \frac{F_2}{1 + (x_3/h)^\beta},$$

where $\Phi_1, \Phi_2, F_1, F_2, h, \beta > 0$ are constants. Obviously,

$$0 < \Phi_1 \leq \Phi(\cdot) < \Phi_1 + \Phi_2, \; 0 < F_1 < F(\cdot) \leq F_1 + F_2.$$

III. Hybrid state estimation in the IGO

In order to estimate the state vector of system (3), a hybrid observer is introduced in [16] as

$$\begin{aligned} \dot{\hat{\mathrm{x}}}(t) = A\hat{\mathrm{x}}(t) + K(\mathrm{y}(t) - \hat{y}(t)), \quad \hat{y}(t) = L\hat{\mathrm{x}}(t), \\ \hat{z}(t) = C\hat{\mathrm{x}}(t), \quad \hat{t}_n < t < \hat{t}_{n+1}, \end{aligned} \tag{4}$$

$$\hat{\mathrm{x}}(t_n^+) = \hat{\mathrm{x}}(t_n^-) + \hat{\lambda}_n B, \quad \hat{t}_{n+1} = \hat{t}_n + \hat{T}_n, \tag{5}$$

$$\begin{aligned} \hat{\lambda}_n = F(\hat{z}(t_n)), \\ \hat{T}_n = \Phi\left(\hat{z}(\hat{t}_n) + k_d(z(\hat{t}_n) - \hat{z}(\hat{t}_n))\right), \end{aligned} \tag{6}$$

[1]The superscripts "$-$" and "$+$" denote henceforth the left- and right-side limits at t_n, respectively.

where $K \in \mathbb{R}^{3\times 2}$ is the continuous feedback matrix and k_d is the gain in the discrete part of the observer. The observer possesses two design degrees of freedom represented by the gains: The scalar gain k_d directly impacts the discrete dynamics of (4) while K is responsible for continuous linear output error feedback to the estimates $\hat{\mathrm{x}}(t)$.

The continuous output error feedback in the observer acts similarly to the local continuous feedback in a generalized version of the IGO studied in [17]; as demonstrated in [17], such a local feedback can destroy positivity of the state vector. The state estimate positivity of hybrid observer (4) is not implied by the positivity of the IGO. However, such a positivity can be guaranteed for a special choice of K, as implied by the following proposition.

Proposition 1 (Positivity): Let the continuous observer gain matrix in observer (4) have the following structure

$$K = \begin{bmatrix} 0 & 0 \\ k_{21} & 0 \\ k_{31} & k_{32} \end{bmatrix},$$

where $g_2 - k_{31} \geq 0$. Then the estimate $\hat{\mathrm{x}}(t)$ is positive (that is, $\hat{x}_i > 0, i = 1, 2, 3$) if $\hat{\mathrm{x}}(0) > 0$ and $\mathrm{y}(t) > 0, \forall t \geq t_0$.

Noticing that the matrix $D = A - KL$ is Metzler and

$$\dot{\hat{\mathrm{x}}}(t) = D\hat{\mathrm{x}}(t) + K\mathrm{y}(t)$$

between the jumping instants, the proof retraces the proof of solution's positivity for the IGO [4] and is omitted here.

The observer (4) possesses more complex dynamics than the IGO. Indeed, the observer dynamics are entrained by the oscillations of the plant or, when the observer pulsatile feedback fires simultaneously with that of the plant, synchronized with them. Such a coupling between oscillators [18], [19] often leads to chaotic and quasiperiodic solutions.

The condition of Proposition 1 does not guarantee convergence of the state estimates, and the additional constraints $b_2 + k_{21} > 0$, $b_3 + k_{32} > 0$ are required to make the matrix D Hurwitz. In fact, even the gain matrices K that result in (slightly) non-Hurwitz matrices D can still produce stable hybrid dynamics through the stabilizing action of k_d, as the continuous and discrete observer dynamics interact. Notice that the observer is functional even with zero values of either gain. The case of $k_d = 0$ is considered in [15] and suffers from slow convergence since the discrete observer dynamics are not corrected by the output error feedback and converge on their own, i.e. unforced. The gain K is instrumental in assigning the convergence rate of the estimation error in the continuous states but not necessary as A is Hurwitz.

IV. Hybrid observer design problem

The dynamics of the IGO are highly nonlinear, so the hybrid state observation problem is solved here with respect to a particular orbit or attractor of the plant. Since no modeling uncertainty is assumed, reconstructing a trajectory is equivalent to estimating the unknown initial condition $(\mathrm{x}(0), t_0)$, though we do not address this problem explicitly.

Let $(\mathrm{x}(\cdot),\,\{t_n\})$ be a solution of (3) that undergoes jumps at the time instants t_n, $n \geqslant 0$. Denoting $\mathrm{x}_n = \mathrm{x}(t_n^-)$,

$$\mathrm{x}(t_n^+) = \mathrm{x}_n + \lambda_n B, \quad t_{n+1} = t_n + T_n$$
$$T_n = \Phi(z(t_n)), \quad \lambda_n = F(z(t_n)),$$

The solution $(\hat{\mathrm{x}}(\cdot),\,\{\hat{t}_n\})$ of (4)–(6) subject to the initial conditions $\hat{t}_0 = t_0$, $\hat{\mathrm{x}}(\hat{t}_0^-) = \mathrm{x}(t_0^-)$, yields $\hat{\mathrm{x}}(t) = \mathrm{x}(t)$ for $t \geq t_0$. Such a solution of the observer is called its *synchronous mode* [15] with respect to the solution $(\mathrm{x}(\cdot),\,\{t_n\})$ of (3).

Once perturbed, the observer in a synchronous mode has to rapidly return to it. A synchronous mode with respect to $(\mathrm{x}(\cdot),\,\{t_n\})$ is called *locally asymptotically stable* (see [15]) if, for any solution $(\hat{\mathrm{x}}(t),\,\hat{t}_n)$ of (4)–(6) such that the initial estimation errors $|\hat{t}_0 - t_0|$ and $\|\hat{\mathrm{x}}(\hat{t}_0^-) - \mathrm{x}(t_0^-)\|$ are sufficiently small, it follows that $\hat{t}_n - t_n \to 0$ and $\|\hat{\mathrm{x}}(\hat{t}_n^-) - \mathrm{x}(t_n^-)\| \to 0$ as $n \to \infty$. This also implies $\hat{\lambda}_n - \lambda_n \to 0$ as $n \to \infty$.

Observing an m-*cycle*, i.e. a periodic solution $(\mathrm{x}(\cdot),\,\{t_n\})$ to (3) with exactly $m \geq 1$ pulses within the least period, is of special interest. To emphasize that a solution to the IGO (respectively, the observer) is an m-cycle, the notation $\mathscr{C}^m(\mathrm{x}(\cdot), \{t_n\})$ and $\mathscr{C}^m(\hat{\mathrm{x}}(\cdot), \{\hat{t}_n\})$ is introduced.

Consider the following hypercube in $\mathbb{R}^3$

$$\mathscr{Z} = [V_1, H_1] \times [V_2, H_2] \times [V_3, H_3],$$
$$V_1 = \frac{F_1}{\mathrm{e}^{b_1(\Phi_1+\Phi_2)} - 1}, \quad V_2 = \frac{g_1 V_1}{b_2}, \quad V_3 = \frac{g_1 g_2 V_1}{b_2 b_3},$$
$$H_1 = \frac{F_1 + F_2}{1 - \mathrm{e}^{-b_1\Phi_1}}, \quad H_2 = \frac{g_1 H_1}{b_2}, \quad H_3 = \frac{g_1 g_2 H_1}{b_2 b_3}.$$

The set $\mathscr{Z}$ is invariant w. r. t. (3): if $\mathrm{x}(0) \in \mathscr{Z}$, then $\mathrm{x}(t) \in \mathscr{Z}$. Furthermore, this set is an attractor: if $x_i(0) \geq 0\,\forall i$, then the following inequalities hold [4]

$$V_i \leq \liminf_{t\to\infty} x_i(t) \leq \limsup_{t\to\infty} x_i(t) \leq H_i, \quad i = 1, 2, 3. \quad (7)$$

In particular, $\mathscr{Z}$ contains all periodic solutions.

For the solution $\mathscr{C}^m(\mathrm{x}(\cdot), \{t_n\})$, consider the interval

$$\mathcal{T} = \{\theta \in \mathbb{R} : \;\; 0 \leq \theta \leq T_\Sigma\},$$

where $T_\Sigma = \sum_{i=0}^{m-1} T_i$ is the least period of the m-cycle. Hence, $\mathcal{D} = \mathscr{Z} \times \mathcal{T}$ is a space of admissible initial conditions for the observer and can be evaluated beforehand given the parameters of the IGO and those of $\mathscr{C}^m(\mathrm{x}(\cdot), \{t_n\})$.

Now, to solve the state estimation problem in (1),(2), observer (4)–(6) has to guarantee asymptotical convergence of the state estimate to the synchronous mode with respect to $\mathscr{C}^m(\mathrm{x}(\cdot), \{t_n\})$ for all trajectories subject to $(\mathrm{x}(0),\, t_0) \in \mathcal{D}$.

While the same observer gain values K, k_d can produce convergence of the estimates with respect to several attractors (e.g. cycles of different multiplicity), this cannot generally be guaranteed in the considered observer structure.

V. Pointwise mapping

Bifurcation analysis of hybrid systems, where continuous dynamics interacts with discrete events, is computationally heavy when direct integration of the system equations is used. The accuracy of the computations is also impacted by the presence of both relatively slow and fast changes in the solutions. A standard way of analyzing hybrid systems makes use of discrete mappings that describe the system evolution from one discrete event to the next one. The mapping introduced in [20] captures the propagation of the continuous observer states through the discrete cumulative (plant and observer) sequence of the feedback firing instants

$$Q : \begin{bmatrix} \hat{\mathrm{x}}_n \\ \hat{t}_n \end{bmatrix} \mapsto \begin{bmatrix} \hat{\mathrm{x}}_{n+1} \\ \hat{t}_{n+1} \end{bmatrix}. \quad (8)$$

Denote $R = (1 - k_d)\,C, \quad \alpha(\zeta, \theta) = R\zeta + k_d z(\theta)$ and

$$S_{k,s} = \{(\zeta,\,\theta) : \;\; \zeta \in \mathbb{R}^3,\;\; \theta \in \mathbb{R},\;\; t_k \leq \theta < t_{k+1},\;\; t_s \leq \theta + \Phi(\alpha(\zeta, \theta)) < t_{s+1}\}.$$

To each $(\hat{\mathrm{x}}_n, \hat{t}_n)$, one can uniquely match two points (x_k, t_k) and (x_s, t_s) of the observed system (if $k = s$, these points coincide) such that $t_k \leq \hat{t}_n < t_{k+1}$, $t_s \leq \hat{t}_n + \Phi(\alpha(\hat{\mathrm{x}}_n, \hat{t}_n)) < t_{s+1}$, that is, each point of the observer hybrid state $(\hat{\mathrm{x}}_n, \hat{t}_n)$ belongs to one of the sets $S_{k,s}$. As shown in [20], mapping (8) can be written as

$$\begin{bmatrix} \hat{\mathrm{x}}_{n+1} \\ \hat{t}_{n+1} \end{bmatrix} = Q(\hat{\mathrm{x}}_n,\, \hat{t}_n) = \begin{bmatrix} P(\hat{\mathrm{x}}_n,\, \hat{t}_n) \\ \hat{t}_n + \Phi(\alpha(\hat{\mathrm{x}}_n, \hat{t}_n)) \end{bmatrix}, \quad (9)$$

where P is a piecewise-defined function such that

$$\begin{aligned} P(\zeta, \theta) \;\; &= \;\; P_{k,s}(\zeta, \theta) = \mathrm{e}^{A(\theta + \Phi(\alpha(\zeta,\theta)) - t_s)}\mathrm{x}(t_s^+) + \\ &+ \;\; \mathrm{e}^{D\Phi(\alpha(\zeta,\theta))}\Big[\zeta + F(C\zeta)B - \mathrm{e}^{A(\theta - t_k)}\mathrm{x}(t_k^+)\Big] - \\ &- \;\; \sum_{i=k+1}^{s} \lambda_i \mathrm{e}^{D(\theta + \Phi(\alpha(\zeta,\theta)) - t_i)} B \;\; \forall (\zeta, \theta) \in S_{k,\,s}. \end{aligned}$$

As proven in [20], if the functions Φ and F are C^1-smooth, the same holds for the map Q. To examine local stability of a solution to the observer, the dynamics given by (9) can be linearized along the trajectory $(\hat{\mathrm{x}}_n,\, \hat{t}_n)$.

Stability conditions for m-cycle of observer (4)–(6) $\mathscr{C}^m(\hat{\mathrm{x}}(t), \hat{t}_n)$ satisfying

$$(\hat{\mathrm{x}}_0,\, \hat{t}_0 + T_\Sigma) = Q^{(m)}(\hat{\mathrm{x}}_0,\, \hat{t}_0)$$

can be obtained through analyzing the Jacobian $\mathcal{F}_m = (Q^{(m)})'$ evaluated at the fixed point of the map $Q^{(m)}$. The m-cycle is locally asymptotically stable if and only if $\mathcal{F}_m$ is Schur stable [15], [20]. The calculation of the Jacobian can be simplified by applying the chain rule, as

$$\mathcal{F}_{n+1} = \hat{J}_n \mathcal{F}_n, \;\; \forall n \geq 0, \quad \mathcal{F}_0 = I, \quad \hat{J}_n = Q'(\hat{\mathbf{x}}_n, \hat{t}_n).$$

For a synchronous mode, $(\hat{\mathrm{x}}(t), \hat{t}_n) = (\mathrm{x}(t), t_n)$, and thus

$$Q'(\hat{\mathrm{x}}_n, \hat{t}_n) = Q'(\mathrm{x}_n, t_n) = J_n = \begin{bmatrix} (J_n)_{11} & (J_n)_{12} \\ (J_n)_{21} & (J_n)_{22} \end{bmatrix}, \quad (10)$$

where the blocks are defined as follows

$$\begin{aligned} (J_n)_{11} &= \Phi'(C\mathrm{x}_n) A x_{n+1} R + \mathrm{e}^{D\Phi(C\mathrm{x}_n)}\,(I + F'(C\mathrm{x}_n)BC)\,, \\ (J_n)_{12} &= A\mathrm{x}_{n+1}(1 + \Phi'(C\mathrm{x}_n) k_d C A \mathrm{x}_n) \\ &\quad - \mathrm{e}^{D\Phi(C\mathrm{x}_n)} A(\mathrm{x}_n + \lambda_n B), \\ (J_n)_{21} &= \Phi'(C\mathrm{x}_n) R, \quad (J_n)_{22} = 1 + \Phi'(C\mathrm{x}_n) k_d C A \mathrm{x}_n. \end{aligned}$$

VI. Bifurcation analysis

In order to discern the mechanisms of the transition from asynchronous to synchronous mode, dynamics of observer (4)-(6) are investigated in this section specifically with respect to variation in the observer gain k_d selected as a bifurcation parameter. The continuous gain matrix is set to

$$K = k_c \begin{bmatrix} 0 & 0 \\ 1 & 0 \\ 0 & 1 \end{bmatrix}, \quad k_c > 0. \tag{11}$$

Then the matrix $D = A - KL$ is Hurwitz as well as Metzler and the continuous state estimate is positive (Proposition 1).

As the analysis below demonstrates, there is a well-defined interval of the gain values that correspond to a synchronous mode of the observer with a sufficient basin of attraction and convergence rate. For the sake of numerical analysis, assume the following parameter values: $b_1 = 0.018$, $b_2 = 0.15$, $b_3 = 0.1$, $g_1 = 2.8$, $g_2 = 1.5$, $\Phi_1 = 40.0$, $\Phi_2 = 80.0$, $F_1 = 0.05$, $F_2 = 5.0$, $h = 2.7$, and $\beta = 2$. Then plant (3) has a stable 2-cycle, see Fig. 1.

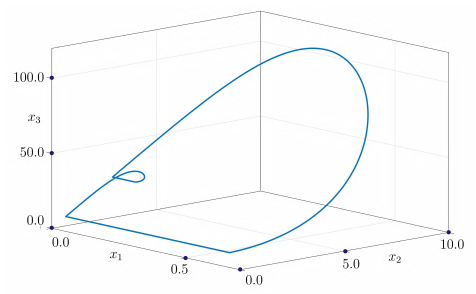

Fig. 1: Three-dimensional phase portrait for the stable 2-cycle with $t_0 = 0$, $T_0 = 119.47, T_1 = 111.05, T_\Sigma = 230.52$

The one-dimensional bifurcation diagram in Fig. 2(a) provides a general overview of the nonlinear observer dynamics. For the values of $k_d < k_d^{\rm sn}$, mapping (9) shows a pair of asynchronous 2-cycles, one of which is stable (drawn in solid lines and denoted by number 3), while the other, drawn in dashed lines and denoted by number 2, is a saddle one.

As the gain k_d increases, the stable 2-cycle (denoted by number 3) merges with the saddle 2-cycle (marked by number 2) and disappears in a saddle-node bifurcation at the point $k_d^{\rm sn}$ (see Fig. 2(a)). The variation of the multipliers $\rho_{1,2}$ and $\rho_1^{\rm u}$ for the stable 2-cycle is shown in Fig. 2(b): with the increasing gain k_d, the stable focus 2-cycle transforms into the stable node 2-cycle, as a pair of complex-conjugate multipliers $\rho_{1,2} = \mu \pm i\omega$ for the stable 2-cycle become real ρ_1 and ρ_2. At the saddle-node bifurcation point $k_d^{\rm sn}$, the largest (in the absolute value) multipliers ρ_1 and $\rho_1^{\rm u}$ of the stable and saddle 2-cycles become equal to $+1$.

When the gain factor k_d passes the value $k_d = k_d^{\rm sn}$, an abrupt transition to chaos takes place, as evidenced by Fig. 2(a), and the observer does not exhibit stable periodic dynamics in the interval between the points $k_d^{\rm sn}$ and $k_d^{\rm sn*}$. In the region $k_d^{\rm sn} < k_d < k_d^{\rm sn*}$, the largest Lyapunov exponent Λ_1 becomes positive, signaling the development of chaotic dynamics, Fig. 2(c). The second Lyapunov exponent Λ_2 remains negative everywhere for $-150.0 < k_d < 100.0$.

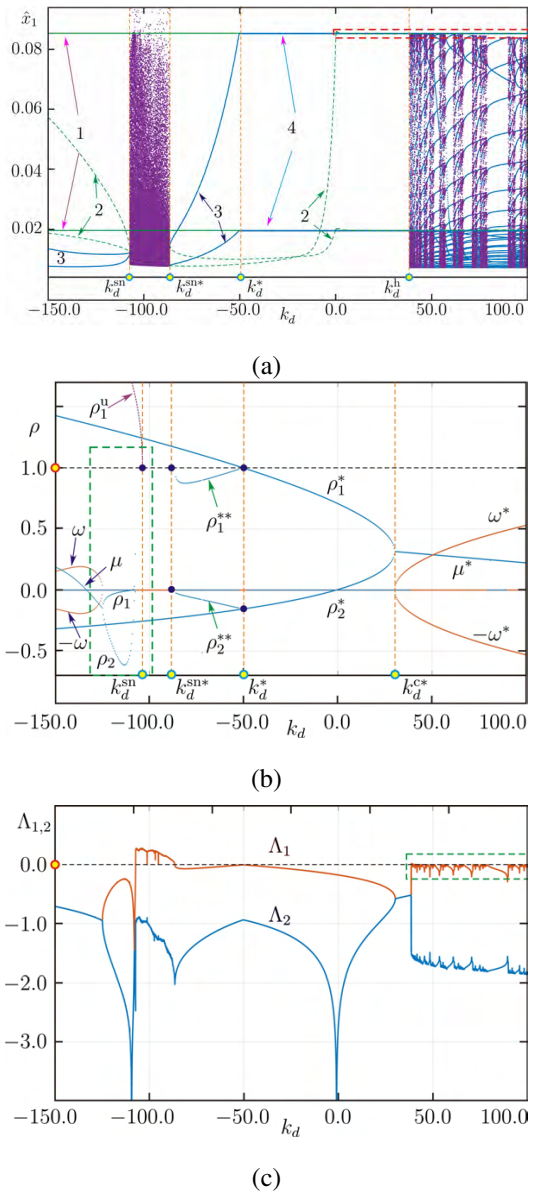

Fig. 2: (a) The transition from a stable asynchronous 2-cycle to an attracting synchronous mode as the discrete gain k_d is increased. The domain between the points $k_d^{\rm h}$ and $k_d = 100.0$ is a region of bistability. Here $k_d^{\rm sn}$ and $k_d^{\rm sn*}$ are the saddle-node bifurcation points. The point k_d^* defines the value of k_d for which a stable synchronous 2-cycle appears. The green dashed lines mark the saddle asynchronous 2-cycles. (b) Multiplier diagrams for the stable synchronous an 2-cycle. The red lines denote the imaginary parts of complex-conjugated multipliers. (c) The two largest Lyapunov exponents $\Lambda_{1,2}$ as functions of k_d.

With the further increase of k_d, the system enters the 2-cycle window. The saddle-node bifurcation at the left edge $k_d^{\rm sn*}$ of the region $k_d^{\rm sn} < k_d < k_d^{\rm sn*}$ produces the saddle

and stable asynchronous 2-cycles, numbered 2 (dashed line) and 3 (solid line), respectively. When crossing the point k_d^* with increasing k_d, the stable asynchronous 2-cycle merges with the saddle synchronous 2-cycle in a "transcritical"-like bifurcation. Unlike the classical transcritical bifurcation, this transition does not involve the appearance of an unstable asynchronous 2-cycle. After this bifurcation, the saddle synchronous 2-cycle transforms into a stable one (numbered 4). Variation of the multipliers for the synchronous $(\rho_{1,2}^*)$ and asynchronous $(\rho_{1,2}^{**})$ 2-cycles is shown in Fig. 2(b).

As illustrated in Fig. 2(b), when crossing the point $k_d^{\mathrm{c}*}$ with increasing gain parameter k_d, the stable node synchronous 2-cycle turns into stable focus (the real multipliers $\rho_{1,2}^*$ become complex $\rho_{1,2}^* = \mu^* \pm i\omega^*$). The domain that falls to the right of the point k_d^{h} is a region of bistability, where the stable synchronous 2-cycle coexists with chaotic or high-periodic attractors. In the domain of chaotic dynamics, there exists a usual dense set of periodic windows, see Fig. 2(a).

It can be concluded that the basins of attraction of the coexisting motions are delineated by the stable manifold of the saddle asynchronous 2-cycle (numbered 2 in Fig. 2(a)), which appears at the point k_d^{sn} in a saddle node bifurcation. Fig. 2(a) reveals that, as the parameter k_d increases, the saddle asynchronous 2-cycle approaches the stable synchronous 2-cycle, when of the gain factor k_d changes the sign.

In the region of bistability $k_d > k_d^{\mathrm{h}}$, the stable synchronous and saddle asynchronous 2-cycles are very close to each other. Here the observer may choose different motions depending on initial conditions. In particular, if a certain ratio between the radii of basins of attractions and the magnitude of random disturbances takes place then either chaotic or high-periodic dynamics occurs. The observer can also exhibit a hard transition from a stable synchronous 2-cycle to a chaotic or high-periodic attractor and vice versa.

Fig. 3 depicts a three-dimensional phase space projection of the coexisting stable synchronous 2-cycle (denoted by $\mathcal{C}_2$) and stable 31-cycle (denoted by $\mathcal{C}_{31}$) for $k_d = 84.5$.

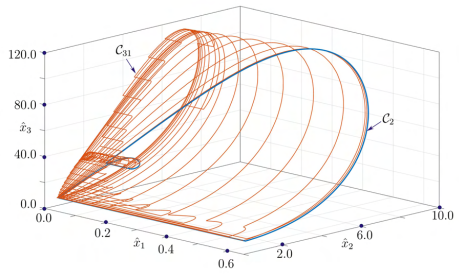

Fig. 3: Coexistence of a stable synchronous 2-cycle (denoted by $\mathcal{C}_2$) and a stable 31-cycle (denoted by $\mathcal{C}_{31}$). $k_d = 84.5$.

VII. Design example

The following bifurcation analysis based iterative algorithm for finding the gains K and k_d for a given periodic mode in the plant $\mathscr{C}^m(\mathrm{x}(\cdot), \{t_n\})$ is proposed. For non-periodic (chaotic, quasi-periodic) trajectories, the design procedure will be the same, replacing the spectral radius of the Jacobian (10) by the maximal Lyapunov exponent.

Initialization: Select the step $\Delta = k_{\max}/N, N \gg 1$. For $k_d = 0$, find the value $k_{\max}$.

do: Starting with $k_c = k_{\max}$ and decreasing k_c with some step Δ do the following (for each fixed k_c)

- **Step 1:** determine the interval $\mathcal{K}$ of the values k_d for which the synchronous mode is locally stable, i.e. the Jacobian is Schur stable
- **Step 2:** exclude the values of k_d for which the stable synchronous mode, according to bifurcation analysis, coexists with other stable modes, obtaining a set $\mathcal{K}_1 \subseteq \mathcal{K}$;
- **Step 3:** find a subset $\mathcal{K}_2 \subseteq \mathcal{K}_1$ such that the whole subspace of feasible initial conditions $\mathcal{D}$ is within the basin of attraction of the synchronous mode;
- **Step 4:** find a subset $\mathcal{K}_3 \subseteq \mathcal{K}_2$ constituted by those k_d for which the settling time $\mathcal{P}(\varepsilon_f) < \mathcal{P}_*$ for all initial conditions from $\mathcal{D}$, where

$$\mathcal{P}(\varepsilon_f) = \hat{t}_{n^*},$$
$$n^* = \min\{n : |\hat{t}_N - t_N| < \varepsilon_f, \forall N > n\}.$$

- **Step 5:** finally, select k_d from $\mathcal{K}_3$ that minimizes the setting time $\mathcal{P}(\varepsilon_f)$.

end:

For the numerical values considered in Section VI, one obtains, with $\varepsilon = 0.02$, that $k_{\max} = 3$. Decreasing k_c with the step $\Delta = 0.1$ (i.e. $N = 30$), the calculations on *Step 1–Step 5* of the proposed above algorithm are performed, for each value of k_c. As a result, one obtains $k_c = 1, k_d = 38.3$ as suitable observer gains.

To illustrate *Step 1–Step 5* of the algorithm in Section 7, the results of one cycle of it for $k_c = 1$ are provided below:

Step 1: the interval $\mathcal{K} = (-49.5, 288.7)$;
Step 2: the interval $\mathcal{K}_1 = (-49.5, k_d^h) = (-49.5, 38.5)$;
Step 3: an analysis of the basin of attraction of the synchronous mode in the four-dimensional initial conditions space reveals that it includes all the points within $\mathcal{D}$ for the interval $\mathcal{K}_2 = \mathcal{K}_1$;
Step 4: for $\mathcal{P}_* = 8000$, one can conclude that the interval $\mathcal{K}_3 = (-25.7, 38.3)$;
Step 5: the averaged over $\hat{t}_0 \in \mathcal{T}$ minimum value of $P(\varepsilon_f)$ for $\varepsilon_f = 1$ is achieved for $k_d = 38.2$.

For the numerical example at hand, the bounds on the hybrid states of the plant are $V_1 = 0.065$, $V_2 = 0.1217$, $V_3 = 1.8275$, $H_1 = 9.84$, $H_2 = 183.7$, $H_3 = 2755$, i.e.

$$\mathcal{D} = \{0.065 \le x_1(0) \le 9.84, \quad 0.1217 \le x_2(0) \le 183.7,$$
$$1.8275 \le x_3(0) \le 2755, \quad 0 \le t_0 \le 230.52\}.$$

The obtained on *Step 5* value of $\mathcal{P}(\varepsilon_f)$ for $k_c = 1$ is minimal for all $0 < k_c \le 3$, so $k_c = 1$ and $k_d = 38.2$ are selected as suitable gain values.

To illustrate the time-domain performance, the designed observer is simulated starting from different initial conditions

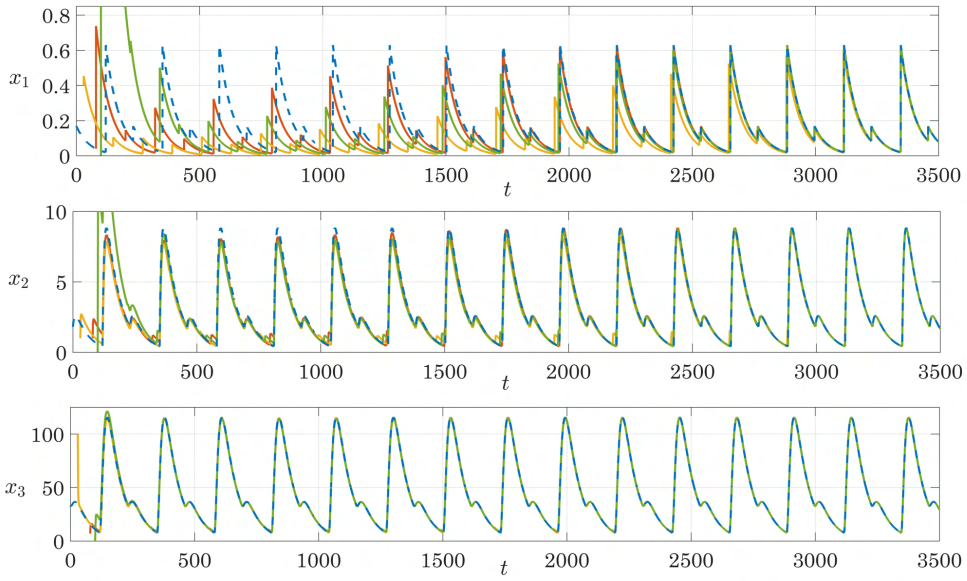

Fig. 4: Transients in the continuous states of the observer due to different initial conditions mismatches with respect to the corresponding plant states (blue dashed lines, $t_0 = 0$). Red lines - initial conditions $\hat{t}_0 = 80, \hat{\mathrm{x}}_0 = [0.04 \;\; 1 \;\; 7]^\top$. Yellow lines - initial conditions $\hat{t}_0 = 30, \hat{\mathrm{x}}_0 = [0.4 \;\; 1 \;\; 100]^\top$. Green lines - initial conditions $\hat{t}_0 = 100, \hat{\mathrm{x}}_0 = [0.001 \;\; 0.01 \;\; 0.01]^\top$.

in Fig. 4. Note that the observer convergence rate does not depend much on the initial conditions for the continuous state estimates. The rate of convergence is affected mostly by the distance $\hat{t}_0 - t_0$ (especially, for cycles of low periodicity, e.g. 1-cycles and 2-cycles, here the influence of k_d is preeminent) and the occurrence of a jump after the first pulse.

VIII. Conclusions

The problem of designing a hybrid observer for the impulsive Goodwin's oscillator is treated, where the discrete state variable is not available for measurement. The observer possesses two design degrees of freedom: a continuous gain and a discrete gain, both implementing feedback of the continuous output estimation error. Due to the complex nonlinear dynamics exhibited by the observer including bistability, high-periodic solutions, and deterministic chaos, a numerical design procedure based on bifurcation analysis is proposed.

References

[1] K. Aihara and H. Suzuki, "Theory of hybrid dynamical systems and its applications to biological and medical systems," *Philosophical Transactions of the Royal Society of London A: Mathematical, Physical and Engineering Sciences*, vol. 368, no. 1930, pp. 4893–4914, 2010.

[2] D. Bainov and P. Simeonov, *Impulsive Differential Equations: Periodic Solutions and Applications*. Harlow, UK: Longman, 1993.

[3] G. T. Stamov, *Almost Periodic Solutions of Impulsive Differential Equations*. Berlin: Springer, 2012.

[4] A. Churilov, A. Medvedev, and A. Shepeljavyi, "Mathematical model of non-basal testosterone regulation in the male by pulse modulated feedback," *Automatica*, vol. 45, no. 1, pp. 78–85, 2009.

[5] B. Goodwin, "Oscillatory behavior in enzymatic control processes," *Nature*, vol. 209, no. 5022, pp. 479–481, 1966.

[6] W. R. Smith, "Qualitative mathematical models of endocrine systems," *Am. J. Physiol.*, vol. 245, no. 4, pp. R473–R477, 1983.

[7] A. Proskurnikov and A. Medvedev, "A simple positive state observer for a generalized Goodwin's oscillator," in *European Control Conference*, Napoli, Italy, 2019, pp. 1671–1676.

[8] P. Mattsson and A. Medvedev, "Modeling of testosterone regulation by pulse-modulated feedback: an experimental data study," in *2013 Int. Symp. Comput. Models Life Sci., AIP Conf. Proc.*, vol. 1559. Melville, New York: AIP Publishing, 2013, pp. 333–342.

[9] ——, "Modeling of testosterone regulation by pulse-modulated feedback," in *Advances in Experimental Medicine and Biology: Signal and Image Analysis for Biomedical and Life Sciences*. Springer, 2015, vol. 823, pp. 23–40.

[10] Z. Zhusubaliyev, A. Churilov, and A. Medvedev, "Bifurcation phenomena in an impulsive model of non-basal testosterone regulation," *Chaos*, vol. 22, no. 1, pp. 013 121–1—013 121–11, 2012.

[11] L. Glass and M. C. Mackey, *From clocks to chaos*. Princeton University Press, 1988.

[12] H. M. Härdin and J. H. van Schuppen, "Observers for linear positive systems," *Linear Algebra Appl.*, vol. 425, no. 2, pp. 571 – 607, 2007.

[13] J. Back and A. Astolfi, "Design of positive linear observers for positive linear systems via coordinate transformations and positive realizations," *SIAM J. Control Opt.*, vol. 47, no. 1, pp. 345–373, 2008.

[14] B. Brian, J. Wang, and Z. Qu, "Nonlinear positive observer design for positive dynamical systems," in *Proceedings of American Control Conference*, 2010, pp. 6231–6237.

[15] A. Churilov, A. Medvedev, and A. Shepeljavyi, "A state observer for continuous oscillating systems under intrinsic pulse-modulated feedback," *Automatica*, vol. 48, no. 6, pp. 1117–1122, 2012.

[16] D. Yamalova, A. Churilov, and A. Medvedev, "Hybrid state observer with modulated correction for periodic systems under intrinsic impulsive feedback," in *Proc. 5th IFAC International Workshop on Periodic Control Systems (PSYCO'2013)*, Caen, France, 2013, pp. 119–124.

[17] H. Taghvafard, A. Medvedev, A. Proskurnikov, and M. Cao, "Impulsive model of endocrine regulation with a local continuous feedback," *Math Biosci.*, pp. 128–135, Feb 2019.

[18] A. Medvedev, A. V. Proskurnikov, and Z. T. Zhusubaliyev, "Mathematical modeling of endocrine regulation subject to circadian rhythm," *Annual Reviews in Control*, vol. 46, pp. 148–164, 2018.

[19] A. Medvedev, P. Mattsson, Z. T. Zhusubaliyev, and V. Avrutin, "Nonlinear dynamics and entrainment in a continuously forced pulse-modulated model of testosterone regulation," *Nonlinear Dynamics*, vol. 94, no. 2, pp. 1165–1181, October 2018.

[20] D. Yamalova, A. Churilov, and A. Medvedev, "Design degrees of freedom in a hybrid observer for a continuous plant under an intrinsic pulse-modulated feedback," *IFAC–PapersOnLine.*, vol. 48, no. 11, pp. 1080–1085, 2015.